

Zr-rich phases in $\text{Sm}(\text{CoFeCuZr})_z$ magnets

M. F. de Campos¹, S. A. Romero², A. C. Neiva³, J. Trota Filho¹, L. R. Lidizio¹,
H. R. Rechenberg², F. P. Missell^{1,4}

¹ DIMCI/DIMAT - Instituto Nacional de Metrologia, Normalização e Qualidade Industrial-
INMETRO, Rua Nossa Senhora das Graças 50 (Xerém), 25250-020 Duque de Caxias, RJ, Brasil

² Instituto de Física, Universidade de São Paulo, São Paulo, SP, Brasil

³ Depto. de Engenharia Química, Escola Politécnica, Universidade de São Paulo, São Paulo, SP,
Brasil

⁴ Depto. de Física e Química, Universidade de Caxias do Sul, Caxias do Sul, RS, Brasil

Mfcampos@inmetro.gov.br

Keywords: $\text{Sm}(\text{CoFeCuZr})_z$ magnets, intermetallic phases, phase diagrams.

Abstract: $\text{Sm}(\text{CoFeCuZr})_z$ commercial magnets are manufactured by powder metallurgy techniques. Microstructural investigations of $\text{Sm}(\text{CoFeCuZr})_z$ magnets have shown that, increasing the Zr content, some impurity phases may appear. An alloy with composition (at%): 60.5% Co – 15.5% Fe – 11.5% Zr - 8.5% Sm - 4% Cu, homogenized at 1050°C, was investigated. Three main phases were identified: rhombohedral 1:3 $(\text{ZrSm})_1(\text{CoFeCu})_3$, hexagonal 1:7 $(\text{SmZr})_1(\text{CoFeCu})_7$ and cubic 6:23 $(\text{Zr})_6(\text{CoFe})_{23}$. Knowledge of possible phases present in 2:17-type magnets allows a better understanding of the nanocrystalline microstructure responsible for high coercivity of these magnets.

1. Introduction

Sintered magnets of the 2:17 type, the so-called $\text{Sm}(\text{CoFeCuZr})_z$ magnets, are used in a wide range of applications, which include microwave power tubes and particle accelerators like synchrotron light sources [1].

A recent study [2] pointed out that the presence of impurity phases is related to the decrease of the coercive field in these magnets. When the Zr content of the magnets is increased, several Zr-rich impurity phases can appear [2]. Our objective here is reproducing one of these phases (the quinary phase of Ref. [2]) in an alloy with Zr content much above that of the typical magnets. This phase was found in alloys near permanent magnet compositions by several research groups [2,3]. The correct identification of the possible phases present allows a better understanding of the nanocrystalline microstructure [4,5] and of the coercivity mechanisms of these magnets.

2. Experimental

An alloy with composition (at%): 60.5% Co – 15.5% Fe - 8.5% Sm – 11.5% Zr - 4% Cu was melted in an arc furnace. All elements had a purity of at least 99.9%. The alloy was homogenized with a heat treatment at 1050°C during 8h, after which the sample was quenched down to room temperature.

A detailed characterization of the microstructure was performed in a FEI Quanta 200 scanning electron microscope (SEM) equipped with EDAX and by means of X-ray diffraction (Cu-K α radiation).

3. Results and Discussion

3.1 Microstructure

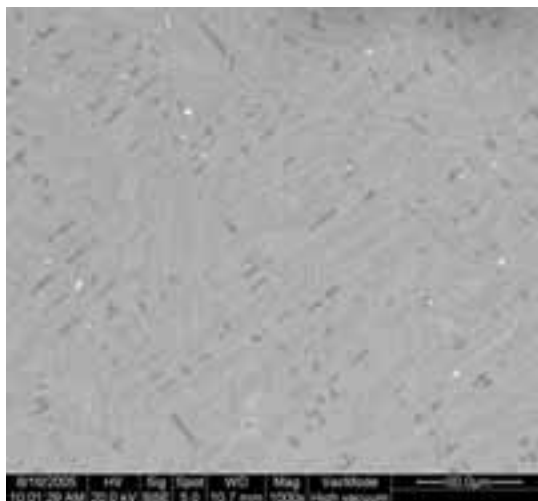


Figure 1. General view of the sample microstructure.

Detailed analysis of the microstructure (see Figs. 1 to 4 and Tables 1 and 2) showed the presence of three main phases. The most abundant is the light grey phase (A). The other important phase is the grey phase (B). We also note a dark phase (C) which always appears surrounded by the light grey phase. EDAX analysis (see Tables 1 and 2) indicates that the light grey phase (A) is probably $(\text{ZrSm})_1(\text{CoFeCu})_3$ (more specifically, the data suggest a stoichiometry close to $(\text{Zr}_{0.67}\text{Sm}_{0.33})_1(\text{CoFeCu})_3$). The grey phase (B), which is the poorest in Zr, appears to be the 1:7 phase $(\text{SmZr})_1(\text{CoFeCu})_7$. The high iron content of the (B) phase seems to help stabilize this structure. The dark phase, which is poor in Sm and Cu is possibly $\text{Zr}_6(\text{CoFe})_{23}$. These phase identifications were confirmed by X-ray diffraction data, to be discussed below.

The above results suggest that the composition of our alloy (60.5% Co – 15.5% Fe – 11.5% Zr - 8.5% Sm - 4% Cu) is inside a 3-phase field of the quinary phase diagram Sm- Zr-Co- Fe-Cu. It is noteworthy that our light grey phase (A) has a composition very similar to the phase - 59.2 Co, 12.6 Fe, 16.6 Zr, 7.4 Sm, 4.2 Cu at.% - reported by Ray and Liu [6]. It is quite plausible that this 1:3 phase (A) is the so-called “platelet” or “lamellae” 1:3 phase mentioned by Rabenberg et al. [7]. The phase $\text{Zr}_6(\text{CoFe})_{23}$ may also appear as an impurity phase in magnets: Makridis et al [8] recently reported the presence of the cubic 6:23 phase in 2:17-type magnets.

Table 1. EDAX analysis for the points indicated in Figure 2a (at%)

| | 1 | 2 | 3 | 4 | 5 | 6 | 7 | 8 | 9 | 10 |
|-----|-------|-------|-------|-------|-------|-------|-------|-------|-------|-------|
| ZrL | 15.98 | 2.72 | 15.77 | 20.38 | 15.85 | 2.26 | 17.73 | 15.91 | 16.35 | 2.84 |
| SmL | 7.64 | 10.17 | 7.33 | 1.03 | 7.53 | 10.51 | 4.79 | 7.56 | 7.52 | 9.95 |
| FeK | 16.57 | 26.91 | 16.56 | 22.09 | 16.42 | 27.29 | 18.47 | 16.82 | 16.48 | 27.14 |
| CoK | 56.50 | 55.40 | 56.72 | 55.47 | 57.06 | 55.33 | 56.38 | 56.30 | 56.37 | 55.46 |
| CuK | 3.33 | 4.80 | 3.61 | 1.02 | 3.14 | 4.60 | 2.63 | 3.41 | 3.28 | 4.61 |

Points 1,3,5,8,9: light grey phase (A). Points 2, 6, 10: grey phase (B). Point 4: dark phase (C) .

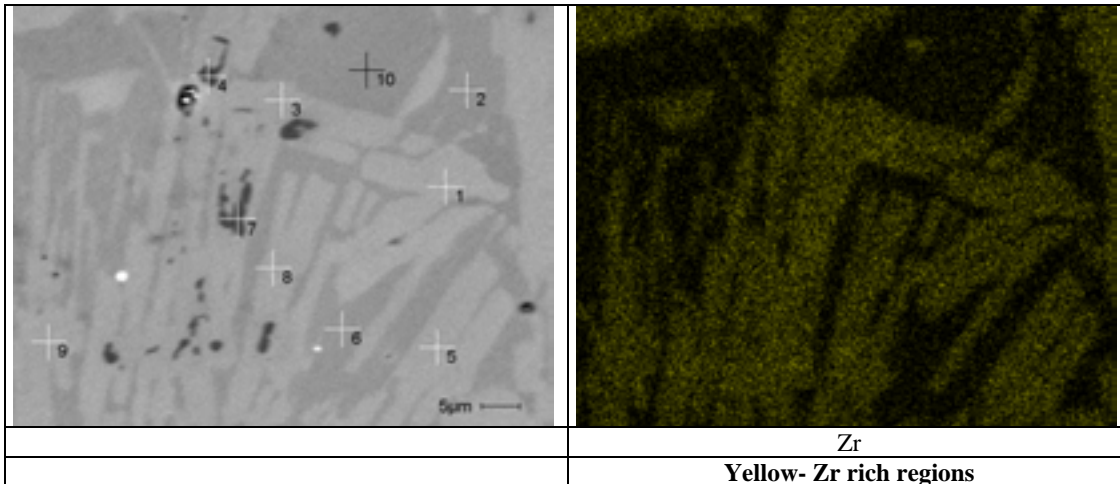


Figure 2. a) Region submitted to microanalysis, indicating the points where EDAX analysis was performed (see Table 1). b) Composition map for the element Zr in this region.

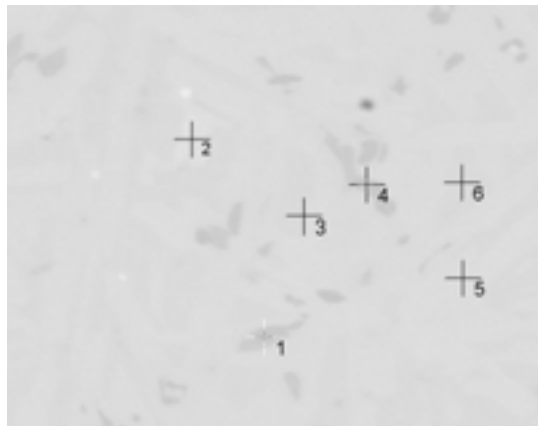


Figure 3. Region submitted to microanalysis, indicating the points where EDAX analysis was performed (see Table 2).

Table 2. EDAX analysis for the points indicated in Figure 3 (at%)

| | 1 | 2 | 3 | 4 | 5 | 6 |
|-----|-------|-------|-------|-------|-------|-------|
| ZrL | 20.69 | 1.99 | 3.59 | 20.62 | 15.42 | 2.16 |
| SmL | 1.23 | 13.16 | 10.60 | 1.42 | 7.68 | 10.34 |
| FeK | 19.64 | 20.28 | 24.06 | 19.59 | 15.49 | 25.03 |
| CoK | 56.39 | 55.26 | 56.45 | 56.77 | 58.12 | 57.46 |
| CuK | 2.05 | 9.30 | 5.30 | 1.61 | 3.29 | 5.01 |

Points 1 and 4 correspond to the dark phase (C) (6:23). Point 5 is the light grey phase (A) (1:3). Points 3 and 6 are the 1:7 phase (B). The Point 2 is a Cu-rich (and also Sm-rich) unidentified phase.

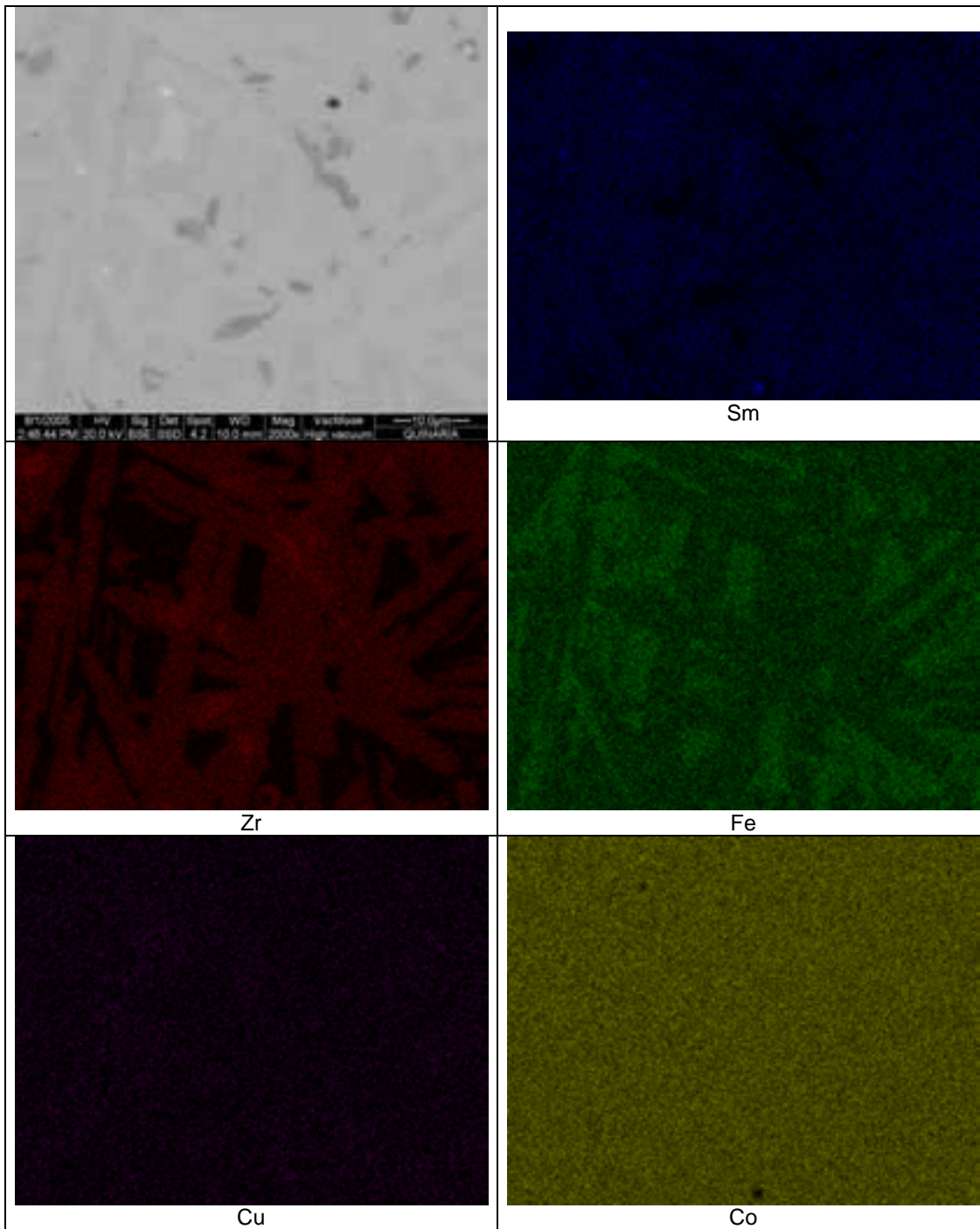


Figure 4. Element map for the region displayed in Fig. 3.

3.2 X-ray diffraction analysis

X-ray diffraction (see Fig. 5 and Table 3) has corroborated the data of SEM analysis discussed previously. The most relevant peaks showed in Fig. 5 were interpreted according Table 3.

Table 3. Interpretation for X-ray diffraction data shown in Fig. 5

| | | | | | | | | | |
|---------|------|------|----------|------|----------|-----------|----------|------|----------|
| Peak 2θ | 30.1 | 33.5 | 36.5 | 40.3 | 43.2 | 44.0 | 45.2 | 46.6 | 50.1 |
| Phases | 1:7 | 1:3 | 1:3, 1:7 | 6:23 | 1:3, 1:7 | 6:23 | 1:3, 1:7 | 1:3 | 1:3,6:23 |
| Peak 2θ | 62.9 | 63.8 | 65.8 | 67.0 | 70.3 | 81.9 | | | |
| Phases | 1:7 | 1:3 | 1:3,1:7 | 1:3 | 6:23 | 1:7, 6:23 | | | |

X-ray diffraction data has confirmed that two main phases are present: Phase (A), rhombohedral $(\text{ZrSm})_1(\text{CoFeCu})_3$, with space group 166, R-3m, hR12, the same structure as PrCo_3 or CeCo_3 . As a consequence of the significant substitution of Sm by Zr, the lattice parameters are smaller than those expected for the binary SmCo_3 compound. Phase (B) is $(\text{SmZr})_1(\text{CoFeCu})_7$ with space group 191, P6/mmm, hR8, (TbCu_7 structure).

Phase (C), cubic $\text{Zr}_6(\text{CoFe})_{23}$, with space group 225, Fm3m, cF116, ($\text{Th}_6\text{Mn}_{23}$ structure) also may be identified, but with a small volume fraction. This is compatible with the microstructures shown in Figs. 1, 2, 3 and 4. The presence of 6:23 is expected from the binary Zr-Co and Zr-Fe diagrams, where cubic 6:23 is a stable phase.

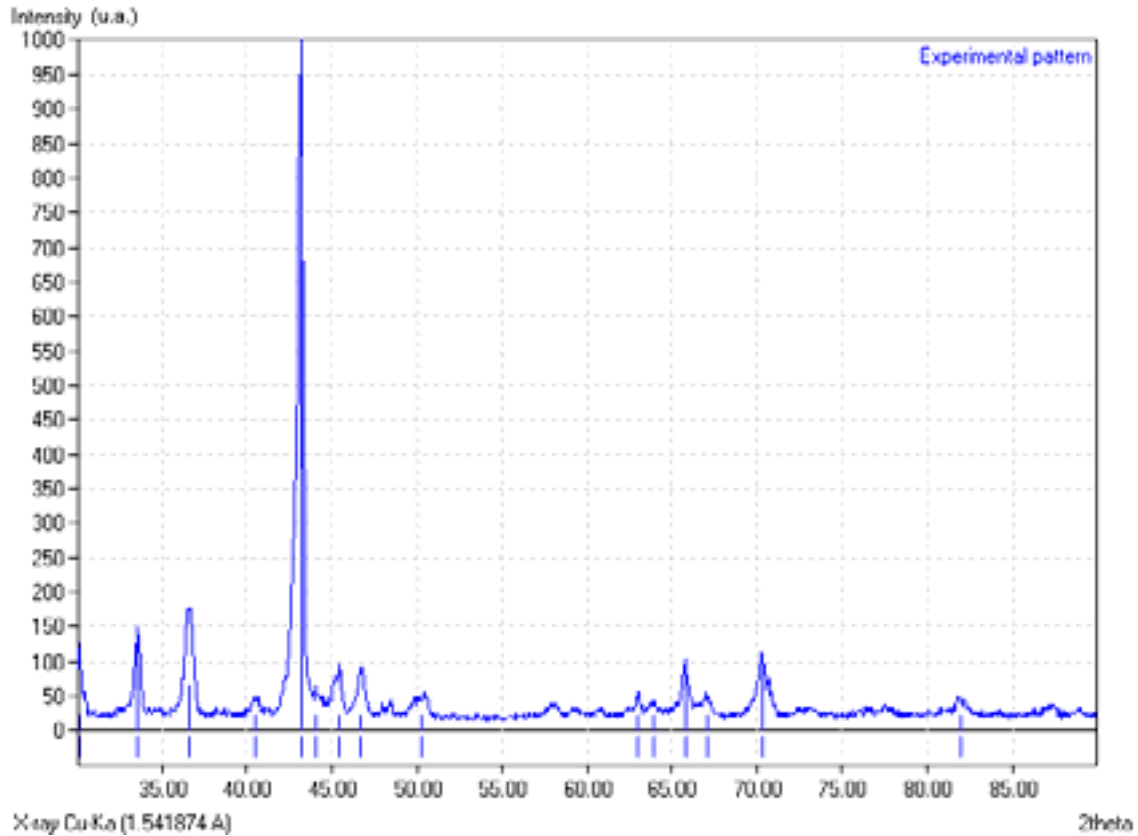


Figure 5. X-ray diffraction spectrum ($\text{CuK}\alpha$ radiation).

3.3 Some Comments

It is believed that, when an impurity phase rich in Zr appears in the microstructure, this implies a loss of Zr from the 2:17 matrix phase, which is unfavorable for the coercivity of the

magnets. This reasoning is based on the experimental observations which indicate that Zr increases the anisotropy field of the 2:17 phase [9].

The Zr-rich 1:3 phase (A) can be the platelet phase [7], which precipitates inside nanocrystalline grains of 2:17 [3-7]. Xiong et al [10] have reported that the Zr content inside the platelet phase increases with the time of heat treatment, and this is another piece of evidence indicating that rhombohedral $(\text{Zr}_{0.66}\text{Sm}_{0.33})_1(\text{CoFeCu})_3$ is probably the lamellae phase.

Conclusions

The two main phases in the sample with composition (at%): 60.5% Co – 15.5% Fe – 11.5% Zr - 8.5% Sm - 4% Cu, homogenized at 1050°C, are: i) rhombohedral $(\text{ZrSm})_1(\text{CoFeCu})_3$ (more specifically, the data suggests a stoichiometry $(\text{Zr}_{0.67}\text{Sm}_{0.33})_1(\text{CoFeCu})_3$) and ii) hexagonal 1:7 phase $(\text{SmZr})_1(\text{CoFeCu})_7$. As a minor phase, cubic $\text{Zr}_6(\text{CoFe})_{23}$ was also identified. The quinary 1:3 phase found in the present study is in agreement with the report by Ray and Liu [6], and can be the platelet phase mentioned by Rabenberg et al. [7]. Reproducing possible phases that can appear in the 2:17 type magnets allows a better understanding of the evolution of the nanocrystalline microstructure responsible for the high coercivity of these magnets.

Zr-rich impurity phases in the microstructure of magnets result in a loss of Zr from the 2:17 matrix phase. This is unfavorable for the coercivity because Zr increases the anisotropy field of the 2:17 phase [9].

Acknowledgements

This work was partially supported by PROMETRO-CNPq.

References

- [1] K. J. Strnat, Proc. of IEEE 78 (1990), p. 923-946.
- [2] M. F. de Campos, A.C. Neiva, S. A. Romero, H. R. Rechenberg, F.P. Missell, J. Alloys. Compd. (2005), in press.
- [3] A. E. Ray, J. Appl. Phys. 67 (1990), p. 4972-4974.
- [4] M.M. Corte-Real, M.F. de Campos, Y. Zhang, G.C. Hadjipanayis, J.F. Liu, Physica Status Solidi (a) 193 (2002), p. 302-313.
- [5] M. F. de Campos, M. M. Corte-Real, Y. Zhang, G. C. Hadjipanayis, J. F. Liu. In: Proc. of 18th International Workshop on High Performance Magnets and their Applications. (Annecy, France, 2004), p. 295-301.
- [6] A.E. Ray, S. Liu, J. Mater. Eng. Perf. 1 (1992), p. 183-192.
- [7] L. Rabenberg, R.K. Mishra, G. Thomas, IEEE Trans. Magn. MAG-19 (1983), p. 2723-2724.
- [8] S. S. Makridis, G. Litsardakis, S. Hofinger, J. Fidler, D. Niarchos. In: Proc. of 18th International Workshop on High Performance Magnets and their Applications. (Annecy, France, 2004), p. 287-294.
- [9] M.V. Satyanarayana, H. Fuji, W.E. Wallace, J. Appl. Phys. 53 (1982), p. 2374-2376.
- [10] X.Y. Xiong, T. Ohkubo, T. Koyama, K. Ohashi, Y. Tawara, K. Hono, Acta Mater. 52 (2004), p. 737-748.